

Magnetic configurations in exchange-biased double superlattices

S. G. E. te Velthuis,^{a)} G. P. Felcher, J. S. Jiang, A. Inomata, C. S. Nelson, A. Berger, and S. D. Bader

Argonne National Laboratory, Argonne, Illinois 60439

(Received 17 August 1999; accepted for publication 2 November 1999)

The layer-by-layer magnetization of a “double-superlattice” Fe/Cr(211) exchange-bias junction was determined by polarized neutron reflectometry. An n -layered $[\text{Fe}/\text{Cr}]_n$ antiferromagnetic (AF) superlattice is coupled with an m -layered $[\text{Fe}/\text{Cr}]_m$ ferromagnetic (F) superlattice, to provide a controlled exchange bias. In low magnetic fields, the magnetizations of the two superlattices are collinear. The two magnetized states (along or opposite to the bias field) differ only in the relative orientation of the F and adjacent AF layer. At higher fields, the AF moments flop to the direction perpendicular to the applied field. The structure, thus determined, explains the magnitude of the bias field. © 1999 American Institute of Physics. [S0003-6951(99)03052-1]

Exchange bias was first discovered in 1956 by Meiklejohn and Bean in Co–CoO particle systems.¹ It refers to the occurrence of a unidirectional magnetic anisotropy that manifests itself in shifted hysteresis loops for coupled ferromagnet (F)–antiferromagnet (AF) systems cooled through the Néel temperature in the presence of a magnetic field.¹ Exchange bias is being utilized in applications such as magnetoresistive read heads,² and is being studied extensively in various AF/F systems,^{3–8} but its origin is still unclear.⁹ Typically, the magnitude of the exchange-bias effect differs, with some exceptions,¹⁰ by $\approx 10^2$ between experiment and theory.

Initially, exchange biasing was interpreted as the result of the exchange interaction at AF/F interfaces: the magnitude of the exchange-bias field is given by balancing the gain in Zeeman energy with the energy cost of interfacial exchange when the ferromagnet reverses its magnetization. In the earliest model,¹¹ both F and AF spin structures were assumed to be a rigid sequence of ferromagnetic planes, with a sequence $+ - + -$ (or $- + - +$) for the AF component; the AF/F interface was taken to be atomically flat. Unfortunately, this picture overestimates the bias fields. Subsequent models^{12–14} attempted to address this by invoking roughness at the interface and/or magnetic domain formation in the AF structure. It is impossible to control the interface between a conventional F–AF pair, and the magnetic configuration of a rough interface cannot be unambiguously defined experimentally.

In view of these unresolved issues, an artificial magnetic system where the effect can be examined with minimal materials-related complexities was proposed.¹⁵ This system is a double superlattice consisting of one F superlattice obtained by an epitaxial sequence of Fe and Cr(211) layers, and one AF superlattice obtained similarly but with a different Cr thickness t_{Cr} (since the interlayer exchange coupling oscillates with t_{Cr}). The coupling between the AF and F superlattices is governed by the value of t_{Cr} between the two superlattices. Since the interlayer coupling has an 18 Å period, the coupling between the AF and F superlattices in double-superlattice structures is relatively insensitive to atomic-scale thickness fluctuations. The layered structure is ideal for a

polarized neutron reflectivity (PNR) study for which 18 Å is well within the instrumental resolution.

A prototype sample had a layer sequence $[\text{Fe}(50 \text{ Å})/\text{Cr}(20 \text{ Å})]_5^{\text{F}}/[\text{Fe}(14 \text{ Å})/\text{Cr}(11 \text{ Å})]_{20}^{\text{AF}}$ (see Table I). $t_{\text{Cr}}=20 \text{ Å}$ between the F and AF superlattices, to provide a ferromagnetic intersuperlattice coupling. A uniaxial anisotropy was introduced by epitaxially growing the sample via dc magnetron sputtering onto single-crystal MgO(110) substrates.¹⁶

The magnetization of the sample, normalized to the saturation value, is presented in Fig. 1. The measurements were obtained with a superconducting quantum interference device magnetometer at room temperature and with the field H applied along the easy axis. Above 15 kOe, the magnetic moments of all layers in both superlattices are aligned with H . In decreasing H , the magnetization decreases as the Fe layers in the AF superlattice first enter a spin-flop state, as the AF coupling becomes comparable to the Zeeman energy and then becomes AF aligned. Below 2 kOe, the magnetic moments of all layers are along the easy axis and H . By cycling H well within $\pm 2 \text{ kOe}$, a minor hysteresis loop is measured (Fig. 1, inset), which exhibits an exchange-bias field of $H_E=39 \text{ Oe}$ and a coercive field $H_C=5 \text{ Oe}$. *The bias effect in the double superlattice is obtained simply by align-*

TABLE I. The layer sequence of the double superlattice. The layer thickness, rms interface roughness, and x-ray scattering length density are obtained from the fit of the x-ray reflectivity data. The x-ray scattering length density consists of real and imaginary terms. The neutron scattering length density used in the calculations are given. The neutron scattering length density of Fe contains a nuclear \pm a magnetic term.

Layers	Thickness (Å)	Roughness (Å)	Scattering length density (10^{-6} Å^{-2})	
			X ray	Neutron
Cr	Cap	49	53.2+5.44i	2.97
Fe) Cr) × 5	F	54	58.3+7.53i	8.12±4.40
		17.8	53.2+5.44i	2.97
Fe) Cr) × 20	AF	14.3	58.3+7.53i	8.12±4.68
		12.1	53.2+5.44i	2.97
Cr	Buffer	197	53.2+5.44i	2.97
MgO(110)	Substrate		30.5+0.32i	5.97

^{a)}Electronic mail: tevelthuis@anl.gov

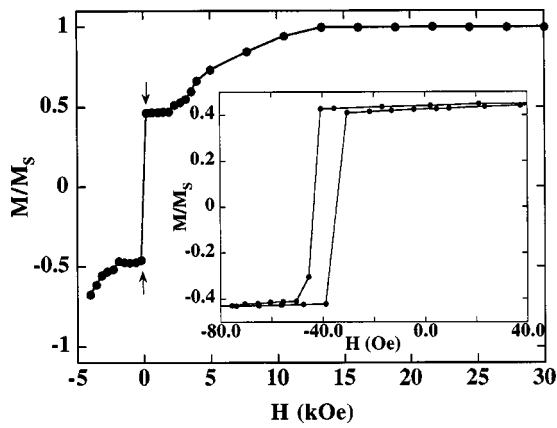


FIG. 1. Partial magnetization curve measured with decreasing field. The arrows indicate the fields for the neutron reflectivity measurements. Inset: The minor hysteresis curve after alignment at 30 kOe.

ing the magnetization of both *F* and *AF* superlattices in high field: this procedure breaks the symmetry between the two energetically degenerate *AF* states and is analogous to field cooling below T_N for conventional *AF-F* systems. Given that the magnetic configuration of the *AF* superlattice is “fixed” and only the magnetization of the *F* superlattice is reversed in the minor hysteresis loop, the magnitude of H_E is equal to that expected on the basis of exchange between collinear superlattices.¹⁵

The first step in the depth profiling is to obtain the x-ray reflectivity with $\text{Cu } K_\alpha$ radiation from a rotating anode x-ray source. The x-ray reflectivity was measured from below the critical angle to above the first *AF* Bragg peak. The structural parameters were obtained via fitting the data to a Parratt model¹⁷ modified to include interface roughness. To reduce the number of free parameters, all *Fe* and *Cr* layers within each superlattice were assumed to have identical thicknesses. In addition, the rms interfacial roughness was assumed to be equal at each *Fe/Cr* interface. The x-ray data and fit are shown in Fig. 2 and the fit parameters are listed in Table I.

The spin-dependent neutron reflectivity gives information about the magnetic and structural profile perpendicular to the surface. R^+ and R^- denote reflectivities for neutrons polarized parallel and antiparallel to H , respectively. The analysis of the data is simple if the magnetization of all layers is collinear with H . R^+ is an optical transform of $n(z)$

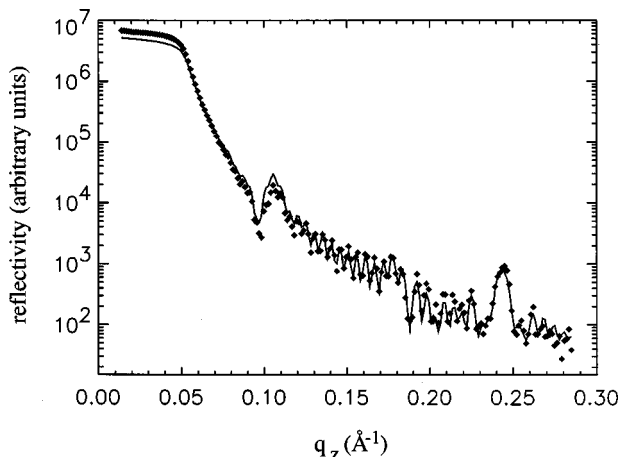


FIG. 2. X-ray reflectivity data (symbols) and fit (curve).

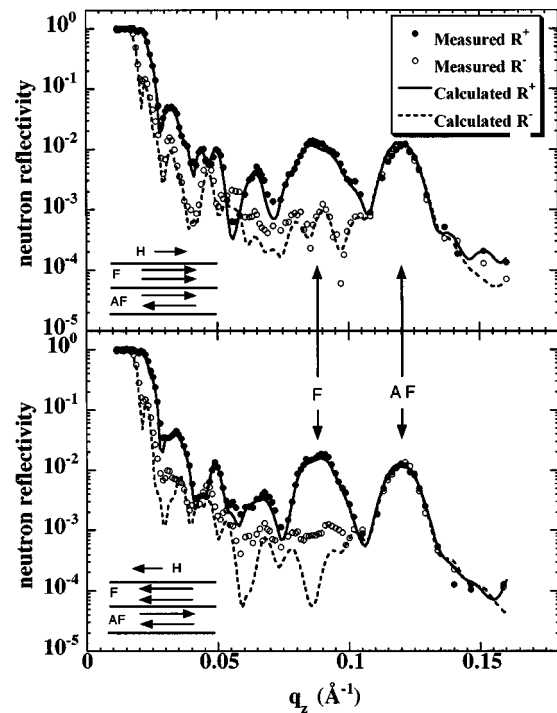


FIG. 3. Measured and calculated polarized neutron reflectivity in $H = 166$ Oe (top) and -72 Oe (bottom). Neutrons with spin parallel to H are indicated by filled symbols/full line (R^+); those antiparallel to H by open symbol/dashed line (R^-).

+ $m(z)$, where n is a depth-dependent nuclear scattering amplitude, and m is the depth-dependent magnetization. R^- is an optical transform of $n(z) - m(z)$. By alternatively measuring with neutrons in either spin state, the magnitude and direction of the layer-by-layer magnetization can be determined.

PNR experiments were performed at Argonne’s Intense Pulsed Neutron Source. Initially, the sample was saturated in $+30$ kOe. Measurements were taken at two opposite magnetization states in the minor loop, at $H = 166$ Oe and $H = -72$ Oe, and at room temperature. The results are shown as a function of momentum transfer (q_z) in Fig. 3.

The large difference in reflectivity for the two spin states indicates that there is a significant magnetization parallel to H . In the low q_z region, the reflectivity becomes unitary at the critical value of the *MgO* substrate. At higher q_z there are two Bragg reflections due to the periodic layer structure of the superlattices. The reflection at $q_z = 0.09 \text{ \AA}^{-1}$ arises from interference between the *Fe* layers in the *F* superlattice. This is clearly a ferromagnetic Bragg reflection because it is extremely spin dependent. The reflection at 0.12 \AA^{-1} arises from the interference between the *Fe* layers within the *AF* superlattice, and corresponds to a periodicity twice that of the structural ordering. Since an equal number of *Fe* layers are magnetized parallel and antiparallel to H , the reflectivities for the two spin states are approximately equal.

The reflectivities for the two magnetic states also show some differences. These do not appear at the critical value (which would mean that the net magnetization is identical in both states), but at larger values of q_z . This shows that some of the Fourier components of the magnetization are indeed different for the two states. However, the problem of uniquely determining the two magnetic depth profiles might

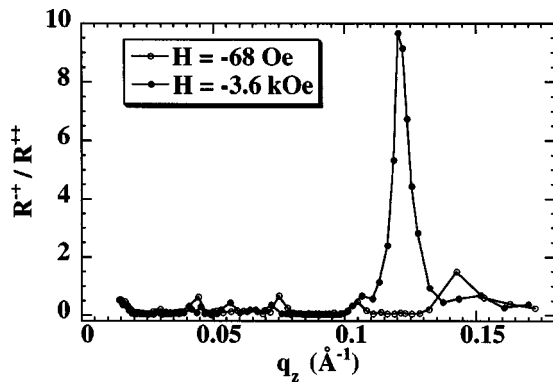


FIG. 4. Ratio between the reflectivity measured for neutrons with the incident spin antiparallel and reflected spin parallel to the field (R^{-+}), and with the incident and reflected spin parallel to the field (R^{++}), in -68 Oe (open symbols) and -3.6 kOe (filled symbols).

seem arduous. Rather than attempting to fit the data, we calculated the reflectivities from: (i) the values for the nuclear scattering length densities for Fe, Cr, and MgO evaluated for the bulk; (ii) structural parameters (layer thicknesses) taken from the best fit of the x-ray reflectivity data; and (iii) the magnetic scattering length density of Fe calculated using the measured magnetizations (1512 and 1609 emu/cm³ for the F and AF superlattices, respectively). Collinear magnetization was assumed for all layers, where the difference between the two states is only in the orientation of the magnetization of the F with respect to the AF superlattice. As illustrated in Fig. 3, not only is there good agreement between experiment and calculation, but the features that distinguish the reflectivities of the two magnetization states are reproduced in the calculations.

In the case of noncollinear magnetizations, PNR can be discussed in a simple way only within the kinematic approximation. The intensity of the AF Bragg reflection is proportional to $R_{AF}^+ = R_{AF}^{++} + R_{AF}^{+-} = (n_{AF}^2 m_{AF,\parallel}^2 + n_{AF}^2 m_{AF,\perp}^2)$ and $R_{AF}^- = R_{AF}^{-+} + R_{AF}^{--} = R_{AF}^+$. n_{AF} is the number of AF layers. m_{AF} is the AF scattering amplitude per layer that originates from the antiparallel components of the sublattice magnetization and $m_{AF,\parallel}$ and $m_{AF,\perp}$ are, respectively, its components parallel and perpendicular to H . Experimentally, they can be separated by analyzing the polarization of the reflected neutrons: $R^{++} = R^{--} = n_{AF}^2 m_{AF,\parallel}^2$ while $R^{-+} = R^{+-} = n_{AF}^2 m_{AF,\perp}^2$. In Fig. 4 the ratio R^{-+}/R^{++} is shown for $H = -68$ Oe and -3.6 kOe. At $H = -68$ Oe, $R^{-+}/R^{++} \approx 0$ at the AF Bragg reflection, indicating a collinear alignment along H . Similarly, no spin-flip reflectivity was observed for a field of -2 kOe. Therefore, there is no evidence of a domain wall in the AF as is predicted by the Mauri¹² and Malozemoff¹³ models. For this system, which is insensitive to interfacial spin frustration, there is a good agreement with the classical Meiklejohn-Bean model.¹¹ Similar results might be obtained for a conventional F-AF pair without interface roughness.

At high fields, -3.6 kOe, $R^{-+}/R^{++} = 9.7$, indicating that the Fe layers in the AF superlattice are still AF ordered,

but now perpendicular to H and to the F superlattice (i.e., flopped). The finite ratio of R^{-+}/R^{++} at -3.6 kOe is amenable to different interpretations. Assuming the system is homogeneous, $R^{-+}/R^{++} = \tan^2 \varphi$, where φ is the angle between the antiparallel components of the AF sublattice magnetization and H . Such an angle ($\approx 70^\circ$ from the easy axis) is not expected for a uniaxial structure with H along the easy axis. A second interpretation is that the sample is made of lateral domains and at $H = -3.6$ kOe a majority, but not all, have flopped. The third and more interesting cause is that the spin-flop transition is not homogeneous along the thickness of the AF superlattice, but is initiated at one end, for instance, at the F/AF interface.

In conclusion, polarized neutron reflectivity demonstrates that in a double superlattice, engineered to provide a controllable exchange bias, the magnetic structure matches that inferred by magnetization measurements,¹⁵ providing a direct link between the microscopic and macroscopic aspects of the magnetism. The two states at either side of the biased hysteresis curve consist of collinear alignments of the Fe magnetization within both superlattices. The difference between the two states originates solely in the orientation (parallel or antiparallel) of the F with respect to the AF superlattice. Furthermore, at high fields the AF superlattice becomes spin flopped with respect to H and the F superlattice. The double superlattice is an exchange-bias system, unhampered by interfacial spin frustrations, yet where field alignment instead of field cooling initiates the bias effect, which exhibits good agreement with theory based on coherent, collinear models.

This work has been supported by U.S. DOE, BES-MS Contract No. W-31-109-ENG-38.

¹W. H. Meiklejohn and C. P. Bean, *Phys. Rev.* **105**, 904 (1957).

²C. Tang, *J. Appl. Phys.* **55**, 2226 (1984)

³J. S. Kouvel, *J. Phys. Chem. Solids* **16**, 132 (1960)

⁴A. E. Berkowitz and J. H. Greiner, *J. Appl. Phys.* **36**, 3330 (1965).

⁵R. Jungblut, R. Coehoorn, M. T. Johnson, C. Sauer, P. J. van der Zaag, A. R. Ball, T. G. S. M. Rijks, J. aan de Stegge, and A. Reinders, *J. Magn. Mater.* **148**, 300 (1995).

⁶T. J. Moran, J. M. Gallego, and I. K. Schuller, *J. Appl. Phys.* **78**, 1887 (1995).

⁷J. Nogués, D. Lederer, T. J. Moran, I. K. Schuller, and K. V. Rao, *Appl. Phys. Lett.* **68**, 3186 (1996).

⁸N. J. Gökemeijer, T. Ambrose, and C. L. Chien, *Phys. Rev. Lett.* **79**, 4270 (1997).

⁹J. Nogués and I. K. Schuller, *J. Magn. Mater.* **192**, 203 (1999).

¹⁰P. J. van der Zaag, A. R. Ball, L. F. Feiner, R. W. Wolf, and P. A. A. van der Heijden, *J. Appl. Phys.* **79**, 5103 (1996).

¹¹W. H. Meiklejohn, *J. Appl. Phys.* **33**, 1328 (1962).

¹²D. Mauri, H. C. Siegmann, P. S. Bagus, and E. Kay, *J. Appl. Phys.* **62**, 3047 (1987).

¹³A. P. Malozemoff, *Phys. Rev. B* **35**, 3679 (1987).

¹⁴N. C. Koon, *Phys. Rev. Lett.* **78**, 4865 (1997); T. C. Schulthess and W. H. Bulter, *ibid.* **81**, 4516 (1998); M. D. Stiles and R. D. McMichael, *Phys. Rev. B* **59**, 3722 (1999).

¹⁵J. S. Jiang, G. P. Felcher, A. Inomata, R. Goyette, C. Nelson, and S. D. Bader (unpublished).

¹⁶E. E. Fullerton, M. J. Conover, J. E. Mattson, C. H. Sowers, and S. D. Bader, *Phys. Rev. B* **48**, 15755 (1993); *J. Appl. Phys.* **75**, 6461 (1994).

¹⁷L. G. Parratt, *Phys. Rev.* **95**, 359 (1954); L. Nevot and P. Croce, *Rev. Phys. Appl.* **15**, 761 (1980).